DOI: 10.17516/1997-1397-2020-13-1-79-86.
УДК 532.517.4

Similarity in the Far Swirling Momentumless Turbulent Wake

Alexey V. Shmidt*
Institute of computational modelling SB RAS
Krasnoyarsk, Russian Federation

Received 14.02.2019, received in revised form 15.10.2019, accepted 20.12.2019

Abstract. A self–similar solution to one model of the far momentumless swirling turbulent wake is proposed in the paper.

Keywords: far swirling turbulent wake, self–similar solution, shooting method.

Citation: A.V.Shmidt, Similarity in the Far Swirling Momentumless Turbulent Wake, J. Sib. Fed. Univ. Math. Phys., 2020, 13(1), 79–86.
DOI: 10.17516/1997-1397-2020-13-1-79-86.

Introduction

Turbulent swirling wakes are usually generated during flow past around a body. Swirls are inserted into the flow by propulsors and they can be formed in various technological devices. An overview of papers devoted to experimental and numerical investigations of the swirling turbulent wakes is presented in [1, 2]. The similarity laws of the swirling turbulent flow decay are investigated [3]. Asymptotic and numerical analysis of the swirling turbulent wakes was performed [4–6]. The classical $k-\varepsilon$ model of turbulence was used in these studies. It was shown that even if the tangential component of the mean velocity is small it significantly affects the flow pattern in the turbulent wake and this influence can be traced at sufficiently large distances behind a body.

The streamwise component of the excess momentum J and angular momentum M are important integral characteristics of the swirling turbulent wake. The case $J = 0$, $M = 0$ corresponds to the swirling turbulent wake behind a self–propelled body. This configuration can be implemented in a wake behind the self–propelled body of revolution (the thrust of a body propulsor compensates the hydrodynamic drag force) with compensation of the swirl introduced by a propulsor.

Numerical modelling of the swirling momentumless turbulent wake ($J = 0$) with nonzero angular momentum was carried out on the basis of the second–order semi–empirical models of turbulence [7–9]. Furthermore, a comparison with experimental data [7] obtained in a wind tunnel in the wake past an ellipsoid of revolution was performed. The drag was compensated by momentum of a swirling jet exhausted from its trailing part and the swirl introduced by the jet was balanced out by the rotation of the body part in the opposite direction.

Experimental results on the swirling turbulent wake for $M \neq 0$ were presented [10–14]. It should be noted that there is a discrepancy in the results obtained by different authors.

*schmidt@icm.krasn.ru

Experimental data on the swirling turbulent wakes with various total excess momentum and angular momentum were presented [11].

The swirling momentumless turbulent wake with nonzero angular momentum was numerically simulated [15–20]. Simulations were based on simplified $e-\varepsilon$ model of turbulence [15, 16] and on the hierarchy of improved semi–empirical second–order models of turbulence [18–20]. Good agreement with experimental data was obtained [11]. Numerical analysis of decay of a swirling turbulent wake corresponding to the case $J = 0$ and $M \neq 0$ was carried out [20]. It was shown that at distances of about 1000 diameters behind the body the flow becomes substantially self–similar. Simplified mathematical models of a far momentumless swirling turbulent wake were constructed and their applicability in the case of large distances from the body was proved.

Self–similar solutions of certain semi–empirical models of free turbulent shear flows were constructed on the basis of group–theoretic analysis and modified shooting method [21–24]. The obtained results are in agreement with the experimental data. In addition to that, a comparison of obtained self–similar solutions of the three–dimensional far momentumless turbulent wake model in a passive stratified medium with results of direct numerical solutions of the complete model was conducted [22]. Moreover, it was found that solutions obtained by the shooting method play the role of an attracting set for solutions obtained by direct numerical calculations of the complete model.

The purpose of this study is to construct self–similar solutions of the simplified model of the far swirling momentumless turbulent wake ($J = 0$, $M \neq 0$) [20] on the basis of the previously developed approach [21–24].

1. Problem statement

In order to demonstrate the flow pattern, a scheme of the experimental set-up (Fig. 1) adapted from [11] is presented. In Fig. 1, the wake develops along x axis, r is the radius, U_0 is the

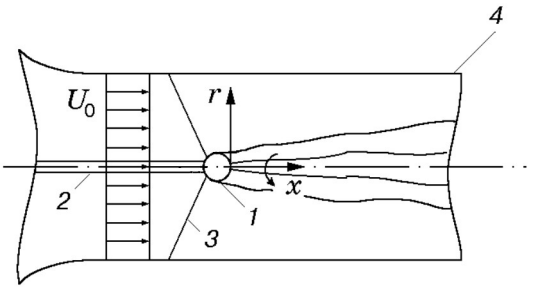

Fig. 1. Scheme of the experimental setup (1 is the sphere, 2 is the tube which delivers the air to form a swirling jet that flows from the rear of the sphere, 3 are tension members, 4 is the throat of the wind tunnel)

undisturbed flow velocity. A special nozzle for a tangential air flow exhausting was built into the trailing edge of the sphere to provide swirling stream behind the sphere.

The following semi–empirical model of turbulence [20] is used to describe the flow in a far momentumless swirling turbulent wake:

$$U_0\frac{\partial U_1}{\partial x} = \frac{1}{r}\frac{\partial}{\partial r}\left(C_u r\frac{e^2}{\varepsilon}\frac{\partial U_1}{\partial r}\right) + \frac{\partial}{\partial x}\int_r^\infty \frac{W^2}{r'}dr', \tag{1}$$

$$U_0\frac{\partial W}{\partial x}=\frac{1}{r^2}\frac{\partial}{\partial r}\left(C_w r^3\frac{e^2}{\varepsilon}\frac{\partial (W/r)}{\partial r}\right), \tag{2}$$

$$U_0\frac{\partial e}{\partial x}=\frac{1}{r}\frac{\partial}{\partial r}\left(C_e r\frac{e^2}{\varepsilon}\frac{\partial e}{\partial r}\right)+C_u r^2\frac{e^2}{\varepsilon}\left(\frac{\partial (W/r)}{\partial r}\right)^2-\varepsilon, \tag{3}$$

$$U_0\frac{\partial \varepsilon}{\partial x}=\frac{1}{r}\frac{\partial}{\partial r}\left(C_\varepsilon r\frac{e^2}{\varepsilon}\frac{\partial \varepsilon}{\partial r}\right)+C_{\varepsilon 1}C_u r^2 e\left(\frac{\partial (W/r)}{\partial r}\right)^2-C_{\varepsilon 2}\frac{\varepsilon^2}{e}. \tag{4}$$

Here $U_1=U-U_0$ is the deficit of the mean longitudinal velocity component, W is the mean tangential velocity component, k is the kinetic energy of turbulence, and ε is the kinetic energy dissipation. It is assumed that the fluid is incompressible and the flow is steady. Moreover, in what follows the undisturbed flow velocity U_0 is taken to be unity. The empirical constants are as follows [20]:

$$C_u=C_w=0.25,\quad C_e=0.147, C_\varepsilon=0.113,\quad C_{\varepsilon 1}=1.44,\quad C_{\varepsilon 2}=1.92.$$

Model (1)–(4) is a simplification of more complicated mathematical model that includes a system of averaged equations of motion, continuity, transport of normal Reynolds stresses and turbulence energy dissipation rate in a rotationally–symmetrical flow in the approximation of a thin shear layer [9, 18, 19, 25]. Moreover, turbulent tangential stresses are determined from nonequilibrium algebraic relations [9, 19, 26]. The simplification introduced in [20] is based on the fact that absolute axial value of the longitudinal velocity component decreases much faster than the maximum absolute value of the tangential velocity component. Therefore, at large distances from the body one can neglect the contribution of this quantity to the term that describes production of turbulence energy . Simplification is based on the far wake approximation and on the replacement of equations for the transfer of normal stresses by a single equation for the turbulence energy balance. In addition, the ratio of the turbulence energy production term to the kinetic energy dissipation is set equal to zero in expressions for turbulent viscosity coefficients (this ratio does not exceed 0.1 in the far wake).

Conservation of total excess momentum and angular momentum follow from equations (1)–(4) and initial and boundary conditions for the considered flow:

$$J=2\pi\rho\int_0^\infty\left(U_0U_1-\int_r^\infty\frac{W^2}{r'}dr'\right)rdr=0, \tag{5}$$

$$M=2\pi\rho\int_0^\infty r^2U_0W dr=M_0\neq 0, \tag{6}$$

here ρ is the fluid density.

It was shown that at large distances behind the body a flow becomes close to self–similar [20]. Therefore, it is natural to seek the self–similar reductions of model (1)–(4).

2. Self–similar reduction

A group analysis is used to construct self-similar solutions [27]. The Lie algebra basis of equations (1)–(4) consists of the following infinitesimal generators:

$$X_1=\frac{\partial}{\partial x},\ X_2=\frac{\partial}{\partial U_1},\ X_3=x\frac{\partial}{\partial x}-2U_1\frac{\partial}{\partial U_1}-W\frac{\partial}{\partial W}-2e\frac{\partial}{\partial e}-3\varepsilon\frac{\partial}{\partial \varepsilon},$$

$$X_4 = r\frac{\partial}{\partial r} + 2U_1\frac{\partial}{\partial U_1} + W\frac{\partial}{\partial W} + 2e\frac{\partial}{\partial e} + 2\varepsilon\frac{\partial}{\partial \varepsilon}.$$

Using the linear combination of operators X_3 and X_4 it is not difficult to obtain the following representation for a solution of the initial model (1)–(4):

$$U_1 = x^{2\alpha-2}U_2(t),\ W = x^{\alpha-1}W_1(t),\ e = x^{2\alpha-2}K(t),\ \varepsilon = x^{2\alpha-3}E(t),\ t = r/x^{\alpha}, \qquad (7)$$

here t is a self–similar variable, α is an arbitrary constant appearing in the linear combination of operators X_3 and X_4.

Using the law of conservation (6) and representation (7) for W, it is not difficult to show that α should be equal to 0.25. Let us remark that decay laws (7) of required functions are in an agreement with the results of numerical calculations of the initial model [20]. They are presented in Fig. 2. In this figure, D is the diameter of a body; $L_{1/2} \sim x^{\alpha}$ is the characteristic scale of the wake width; $|U_{10}|$ is the absolute axial value of the defect of longitudinal velocity component; $|W_m|$ is the maximum absolute value of the tangential velocity component; e_0 is the axial value of kinetic energy of turbulent disturbances; ε_0 is the axial value of kinetic energy dissipation. Markers correspond to experimental data. It can be noted that the decay law of an axial value of the defect of longitudinal velocity component changes at about 1000 diameters behind the body. This is apparently due to the fact that swirl term in equation (1) is negligible at large distances from the body (see, [11]).

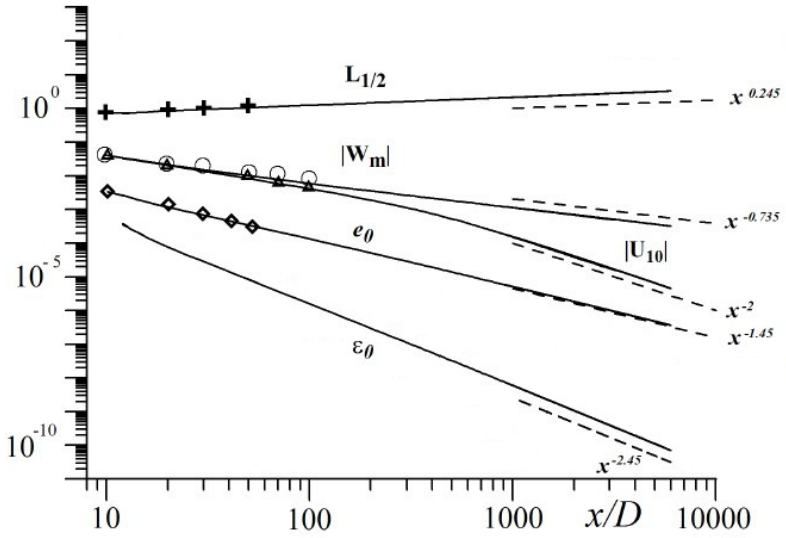

Fig. 2. Variation of dimensionless scale turbulence characteristics in the swirling momentumless wake versus distance from the body

In this case the Lie algebra basis of equations (1)–(4) consists of the following infinitesimal generators:

$$X_1 = \frac{\partial}{\partial x},\quad X_2 = \frac{\partial}{\partial U_1},\quad X_3 = r\frac{\partial}{\partial W},\quad X_4 = x\frac{\partial}{\partial x} - W\frac{\partial}{\partial W} - 2e\frac{\partial}{\partial e} - 3\varepsilon\frac{\partial}{\partial \varepsilon},$$

$$X_5 = U_1\frac{\partial}{\partial U_1},\quad X_6 = r\frac{\partial}{\partial r} + W\frac{\partial}{\partial W} + 2e\frac{\partial}{\partial e} + 2\varepsilon\frac{\partial}{\partial \varepsilon}.$$

Corresponding self–similar representation of solution has the form

$$U_1 = x^{\beta} U_2(t), \quad W = x^{\alpha-1} W_1(t), \quad e = x^{2\alpha-2} K(t), \quad \varepsilon = x^{2\alpha-3} E(t), \quad t = r/x^{\alpha}. \tag{8}$$

Here β is an arbitrary constant. Let us remark that in the self–propulsion mode ($J = 0$, $M = 0$) the mean tangential velocity component decreases much faster (see, [9]).

Using representation (7), we obtain a reduction of initial mathematical model (1)–(4) to the following system of ordinary differential equations:

$$C_u \frac{K^2 U_2''}{E} + \left(C_u \frac{K}{E} \left(2K' - \frac{KE'}{E} + \frac{K}{t} \right) + \alpha t \right) U_2' - 2(\alpha - 1) \left(U_2 + \int_t^{\infty} \frac{W_2^2}{t'} dt' \right) - \alpha W_1^2 = 0, \tag{9}$$

$$C_u \frac{K^2 W_1''}{E} + \left(C_u \frac{K}{E} \left(2K' - \frac{KE'}{E} + \frac{K}{t} \right) + \alpha t \right) W_1' + \left(C_u \frac{K}{E} \left(2K' - \frac{KE'}{E} + \frac{K}{t} \right) - \right.$$
$$\left. - \alpha + 1 \right) W_1 = 0, \tag{10}$$

$$C_e \frac{K^2 K''}{E} + 2C_e \frac{K K'^2}{E} + \left(C_e \frac{K^2}{E} \left(\frac{E'}{E} - \frac{1}{t} \right) + \alpha t \right) K' + C_u \frac{K^2}{E} \left(W_1' - \frac{W_1}{t} \right)^2 +$$
$$+ 2(\alpha - 1) K - E = 0, \tag{11}$$

$$C_\varepsilon \frac{K^2 E''}{E} - C_\varepsilon \frac{K^2 E'^2}{E^2} + \left(C_\varepsilon \frac{K}{E} \left(2K' + \frac{K}{t} \right) + \alpha t \right) E' - C_u C_{\varepsilon 1} K \left(W_1' - \frac{W_1}{t} \right)^2 - C_{\varepsilon 2} \frac{E^2}{K} -$$
$$- (2\alpha - 3) E = 0. \tag{12}$$

For representation (8) the first equation of the reduced system has the following form:

$$C_u \frac{K^2 U_2''}{E} + \left(C_u \frac{K}{E} \left(2K' - \frac{KE'}{E} + \frac{K}{t} \right) + \alpha t \right) U_2' - \beta U_2 = 0. \tag{13}$$

Reduced system (10)–(13) is solved numerically.

3. Calculation results

Solutions of reduced system (10)–(13) have to satisfy the following conditions:

$$U_2'(0) = W_1(0) = K'(0) = E'(0) = 0,$$
$$U_2(a) = W_1(a) = K(a) = E(a) = 0.$$

The first group of conditions takes into account that flow is symmetric with respect to the Ox axis. The second group of conditions follows from the requirement that flow is undisturbed outside the turbulent wake domain (all required functions have to take zero values in this domain). The value of a related with the turbulent wake semi-width can be either set equal to unity in calculations because equations of reduced system (10)–(13) are invariant with respect to the transformation of extension or taken from the experimental data. It should also be noted that coefficients of system (10)–(13) have singularities in boundary conditions.

For numerical solution of the boundary value problem the modified shooting method was used, together with the asymptotic expansion of the solution in the vicinity of the singular point $t = a$

$$U_2 = c_1 |t-a|^{\alpha_1} + o\left(|t-a|^{\alpha_1}\right), \quad W_1 = c_2 |t-a|^{\alpha_2} + o\left(|t-a|^{\alpha_2}\right), \quad K = c_3 |t-a|^{\alpha_3} + o\left(|t-a|^{\alpha_3}\right),$$

$$E = c_4|t-a|^{\alpha_4} + o\left(|t-a|^{\alpha_4}\right), \quad \alpha_3 = \frac{C_\varepsilon}{2C_\varepsilon - C_e}, \quad \alpha_1 = \alpha_2 = \frac{C_e}{C_u}\alpha_3, \quad \alpha_4 = 2\alpha_3 - 1, \quad c_3 = \frac{C_e\alpha_3 c_2^2}{a\alpha}.$$

As the result of calculations the following values were obtained:

$$\beta = -2.09, \quad U_2(0) = 0.35378, \quad W_1'(0) = -0.916, \quad K(0) = 1.14357, \quad E(0) = 1.32668.$$

In Fig. 3 self-similar profiles of solutions obtained by the shooting method are compared with numerical results obtained on the basis of the full model of equations (1)–(4) [20] (1–3 are numerical results [20], 4 are self-similar solutions obtained by the shooting method).

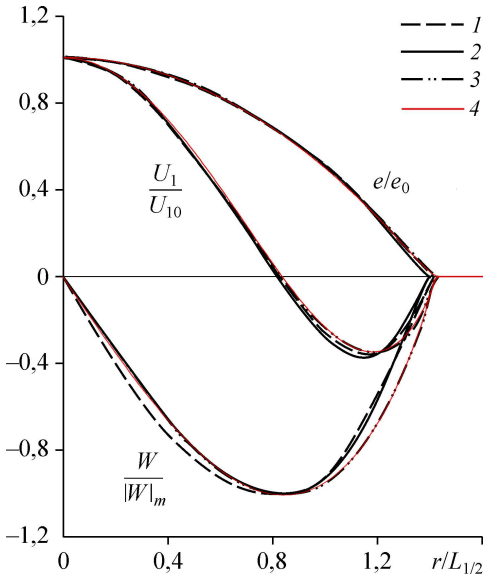

Fig. 3. Self-similar normalized profiles of the deficit of the mean longitudinal velocity component, the mean tangential velocity component, and the kinetic energy of turbulence

Self-similar distributions presented in Fig. 3 are very close to numerical results [20]. Therefore, this indicates the applicability of simplified mathematical models [20] to simulations of the far field of swirling momentumless turbulent wake.

Self-similar profiles of turbulence energy and tangential velocity components are finite bell-shaped functions. At the same time the self–similar profile of the defect of the velocity longitudinal component has regions of negative and positive values. This is in agreement with conservation laws (5) and (6).

The study was supported by the Russian Foundation for Basic Research (grant no. 17-01-00332)

References

[1] J.A.Schetz, Injection and mixing in turbulent flow, *Progr. in Astronautics and Aeronautics*, **68**(1980)

[2] J.Piquet, Turbulent flows. Models and physics, Berlin, Heidelberg: Springer-Verlag, 1999.

[3] A.Reynolds, *J. of Fluid Mech.*, **14**(1962), no. 2, 241–243.

[4] A.G.Gumilevskii, *Fluid Dyn.*, **27**(1992), no. 3, 35–41.

[5] A.G.Gumilevskii, *Fluid Dyn.*, **28**(1993), no. 1, 30–34.

[6] A.G.Gumilevskii, *Fluid Dyn.*, **28**(1993), no. 5, 619–623.

[7] N.V.Gavrilov, A.G.Demenkov, V.A.Kostomakha, et al., *J. of Appl. Mech. and Tech. Phys.*, **41**(2000), no. 4, 619–627.

[8] G.G.Chernykh, A.G.Demenkov, V.A.Kostomakha, **19**(2005), no. 5, 399–408. DOI:10.1080/10618560500228024

[9] A.G.Demenkov, G.G.Chernykh, *Thermophys. and Aeromech.*, **23**(2016), no. 5, 667–675. DOI: 10.1134/S086986431605005X

[10] L.N.Voitovich, An experimental study of swirling turbulent jet flows, In Industrial aerodynamics. Aerodynamics of blade machines, channels and jet flows, Ginevsky A.S. (Ed.), Issue 1 (33), 1986, 224–675 (in Russian).

[11] V.A.Kostomakha, N.V.Lesnova, *J. of Appl. Mech. and Tech. Phys.*, **36**(1995), no. 2, 226–233. DOI: 10.1007/BF02369653

[12] T.Faure, G.Robert, Turbulent kinetic energy balance in the wake of a self–propelled body, *Exp. in Fluids.*, **21**(1996), no. 4, 268–274.

[13] A.I.Sirviente, V.Patel, *AIAA J.*, **38**(2000), no. 4, 620–627. DOI: 10.2514/2.1032

[14] A.I.Sirviente, V.Patel, *AIAA J.*, **39**(2001), no. 12, 2411–2414.

[15] J.A.Schetz, S.Favin, Numerical solution for the near wake of a body with propeller, *AIAA J. of Hydronautics*, **11**(1977), no. 10, 136–141.

[16] J.A.Schetz, S.Favin, *AIAA J. of Hydronautics*, **13**(1979), no. 4, 46–51.

[17] M.H.Lu, A.I.Sirviente, Numerical study of the momentumless wake of an axisymmetric body, 43rd AIAA Aerospace Sciences Meeting and Exhibit, Reno, Nevada: AIAA-2005-1109, 2005. <http://hdl.handle.net/2027.42/77294>

[18] A.G.Demenkov, V.A.Kostomakha, G.G.Chernykh, *J. Comp. Techn.*, **2**(1997), no. 5, 26–34 (in Russian).

[19] G.G.Chernykh, A.G.Demenkov, V.A.Kostomakha, *Russ. J. of Numer. Anal. and Math. Model.*, **13**(1998), no. 4, 279–288.

[20] A.G.Demenkov, G.G.Chernykh, **24**(2017), no. 6, 867–871. DOI:10.1134/S0869864317060051

[21] O.V.Kaptsov, A.V.Shmidt, *SIGMA*, **8**(2012), 073. DOI:10.3842/SIGMA.2012.073

[22] O.V.Kaptsov, A.V.Fomina, G.G.Chernykh, A.V.Schmidt, *Math. Modell.*, **27**(2015), no. 1, 84–98 (in Russian).

[23] O.V.Kaptsov, A.V.Shmidt, *J. of Appl. Math. and Mech.*, **79**(2015), no. 5, 459–466. DOI: 10.1016/j.jappmathmech.2016.03.007

[24] A.V.Shmidt, *J. of Appl. Mech. and Tech. Phys.*, **56**(2015), no. 3, 414–419. DOI 10.1134/S0021894415030104

[25] B.E.Launder, A.Morse, Numerical prediction of axisymmetric free shear flows with a second-order Reynolds stress closure, in: Turbulent shear flows, Springer, Berlin, 1979, 279–294.

[26] W.Rodi, *ZAMM J. of Appl. Math. and Mech.*, **56**(1976), 219–221.

[27] L.V.Ovsyannikov, Group analysis of differential equations, New York, Academic Press, 1982.

Автомодельность дальнего закрученного безымпульсного турбулентного следа

Алексей В. Шмидт
Институт вычислительного моделирования СО РАН
Красноярск, Российская Федерация

Аннотация. В работе проведено построение автомодельного решения полуэмпирической модели дальнего безымпульсного закрученного турбулентного следа.

Ключевые слова: дальний закрученный турбулентный след, автомодельное решение, метод стрельбы.